

# Efficient Modeling of Damage Processes in Heterogeneous Materials under Impact Load

Rajesh S. Kumar, Mark R. Gurvich

United Technologies Research Center

411 Silver Lane, East Hartford, CT 06108, USA

[KumarRS@utrc.utc.com](mailto:KumarRS@utrc.utc.com) , [GurvicMR@utrc.utc.com](mailto:GurvicMR@utrc.utc.com)

*Abstract: A general computational approach for modeling of damage in heterogeneous materials and structures under dynamic load is the focus of the current work. The approach covers processes of both damage initiation and damage propagation. In addition, multiple damage modes are considered to capture complex mechanisms of material failure. The proposed approach is based on selection of two types of expected damage mechanisms, namely, interfacial and internal damage. Interfacial damage is modeled by cohesive elements, while internal damage is analyzed using progressive damage and failure material definitions. Computational implementation in Abaqus/Explicit is illustrated on example of a laminated composite structure. Challenges of robust solutions under impact loading are considered in detail, and efficiency of the implementation is demonstrated. Finally, validation of the generated results is presented via comparison with independent LS-DYNA-based solutions.*

*Keywords: Composite, Heterogeneous Materials, Impact, Fracture, Damage, Crack, Cohesive Elements, Progressive Failure.*

## 1. Introduction

Robust modeling of complex structures under impact loading is, probably, one of the most difficult areas in contemporary FEA for practical engineering applications. Efficient computational analysis of damage processes presents significant challenges especially, for complex crack patterns. Thus, Abaqus/Explicit seems to be an invaluable tool in modeling of damage processes under impact load due to its advanced capabilities to capture both the dynamic nature of loading as well as material failure.

In the case of heterogeneous materials and structures, complexities of internal microstructure and expected damage patterns can require considerable modeling efforts and/or computationally expensive solutions. Modeling of such problems, therefore, has a risk to be reduced into either extremely time-consuming analysis or too simplified statements with limited practical value. Thus, development of computationally efficient, yet physically adequate modeling approaches for heterogeneous materials is valuable in engineering decision making process especially when dealing with complex and large composite and/or hybrid structures.

The objective of this study is to develop a general engineering approach for modeling damage in complex heterogeneous materials and structures under impact load and demonstrate its efficient

computational implementation on a representative example. The developed methodology is expected to capture damage initiation, damage propagation, and the complexity of sophisticated damage network. An additional objective is numerical validation of obtained representative results via independent FEA solutions.

## 2. Approach

Damage processes in heterogeneous materials such as laminated composite materials (Figure 1a) are complex and spans multiple length-scales. Conceptually, damage initiates at the scale of fiber in the form of matrix cracking, fiber-matrix interfacial debonding, and fiber fracture. These microscopic damage entities coalesce to form macroscopic damage within the plies such as longitudinal and transverse ply cracks. In addition, in laminated material system, interfacial damage may occur between the plies leading to delamination. The damage evolution processes are inherently coupled, for example, a delamination typically forms when a transverse ply crack tip reaches the ply interface. Modeling all of these damage processes in an explicit manner is computationally prohibitive. Thus, typically, individual damage mechanism is considered in isolation with the assumption that the coupling is not important.

In the present approach, all expected damage patterns at the simulation length-scale are divided into two basic categories. The first one defines major damage with well-defined spatial locations and growth directions. In the case of heterogeneous materials, interfacial boundaries are obvious candidates for such damage (Figure 1b). Since topology and geometry of expected interfacial damage are perfectly described, they can be easily modeled in FEA by cohesive elements (CE).

The second category defines possible lower length-scale damage mechanisms within the bulk material. These internal damage (Figure 1c) can cover potentially the entire volume of the material, and their locations, orientations and/or geometries are not known *a priori*. In the case of internal damage, therefore, cohesive elements are less efficient. It is suggested to use Progressive Damage (PD) models for FEA of the internal damage as shown in Figure 1d. Different definitions of PD models may be used in principle. For isotropic elasto-plastic materials, ductile or shear PD material models can be used to describe damage initiation and evolution. For anisotropic linear elastic materials such as fiber-reinforced polymer matrix composites, PD model (Hashin damage initiation and evolution) can be applied. For more complex anisotropic non-linear elastic materials such as ceramic matrix composites a user defined subroutine for PD would be required, since available Abaqus capabilities do not support them so far (up to v6.9-1).

The described definition of expected damage patterns as two physically-connected but independently modeled crack networks provides a very convenient way to reduce the complexity of analyses. Firstly, existing FEA meshes can be used to add both interfacial and internal damage. Secondly, possible ambiguity of damage growth is significantly mitigated as major interfacial cracks are easily recognized and taken into account. Finally, the sophisticated nature of multiple cracks is expected to be predicted, so subjectivism in their analysis will be mitigated. The approach can be easily applied for a wide range of materials or structures as illustrated, for example, for fiber-matrix microstructure (Figure 2a) and T-shape composite joint (Figure 2b).

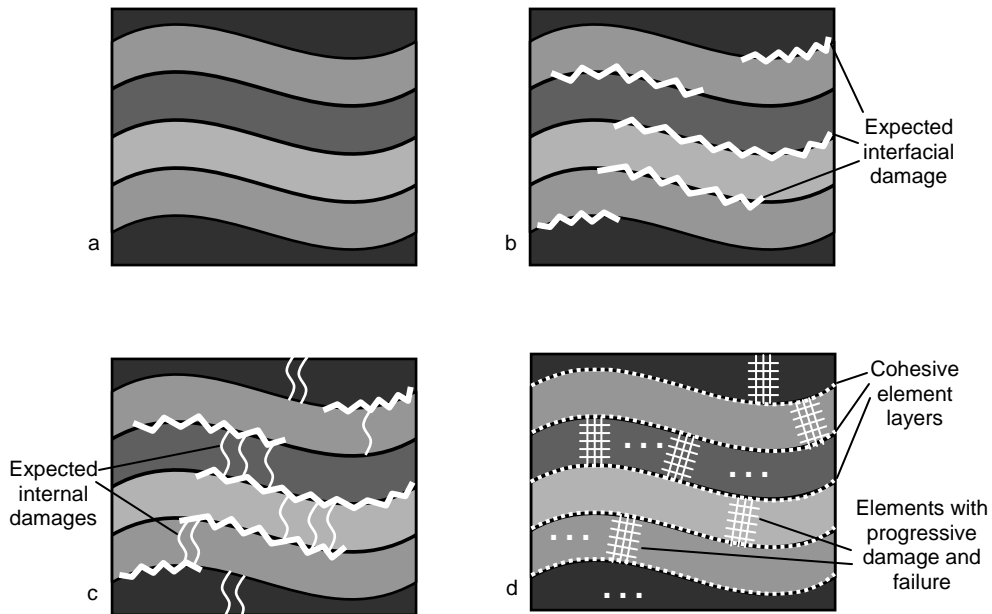


**Figure 1. (a) Schemes of heterogeneous material, (b) expected interfacial damage, (c) expected internal damage, and (d) FEA implementation**

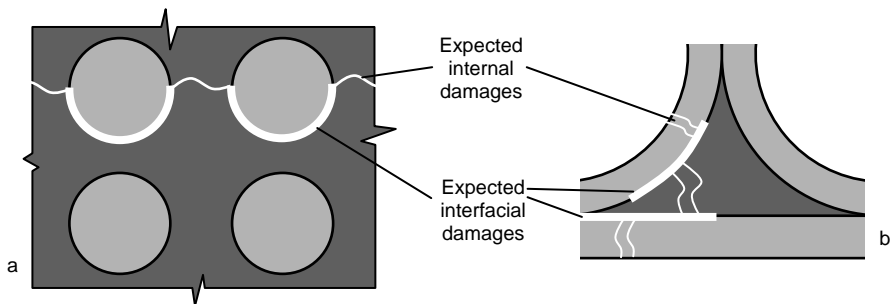


**Figure 2. Examples of damage in heterogeneous materials: (a) micro-structure of fiber-reinforced composites, and (b) T-shape composite joint.**

### 3. Representative Example

In order to illustrate the developed approach of damage formation and growth in heterogeneous materials under dynamic load, a representative curved composite panel shown in Figure 3 is considered. The dimensions of the panel are  $L = W = 200$  mm,  $H = 25$  mm, and  $h = 5$  mm. The two bottom ends of the panel are assumed to be fixed, and a rigid hemispherical impactor of mass 0.1 kg impacts the center of the panel from below (+Y direction). The panel is made of unidirectional plies with the layup of  $[0/90]_{10}$  with the fibers in 0 degrees plies aligned along the global Z-direction and fibers in the 90 degrees plies follow the curvature of the panel. The 20<sup>th</sup> ply of the panel comes into the contact with the impactor first (Figure 3). The following representative material characteristics of plies are used in the simulations: elastic properties ( $E_{11} = 150$  GPa;  $E_{22} = E_{33} = 10$  GPa;  $\nu_{12} = \nu_{13} = 0.25$ ;  $\nu_{23} = 0.45$ ;  $G_{12} = G_{13} = 6$  GPa;  $G_{23} = 4$  GPa); strength properties ( $X_T = X_C = 1400$  MPa;  $Y_T = 40$  MPa;  $Y_C = 250$  MPa;  $S_L = S_T = 60$  MPa); ply fracture energy ( $G_T^f = G_C^f = 14$  MPa-mm;  $G_T^m = 0.2$  MPa-mm;  $G_C^m = 7$  MPa-mm); and density =  $1.6e-9$  tonnes/mm<sup>3</sup>.

A FE model of the panel is developed within Abaqus/CAE. The plies are individually modeled so that cohesive elements may be inserted at each of the nineteen interfaces between the plies. The plies are modeled using continuum shell (SC8R) or solid (C3D8R) elements with one element through the thickness for each ply. The number of elements along the X- and Z- directions is 80. Furthermore, the mesh is biased such that higher mesh density is obtained in the center where the impactor hits the panel (Figure 4). The mesh is selected based on a limited mesh-sensitivity analysis and overall computational resources.

In the models that allow for interfacial damage mechanism, zero thickness CEs (COH3D8) are embedded between each ply. The CEs are such that they share nodes with the elements in the layers above and below them. The cohesive constitutive behavior is specified via triangular traction-separation relationship. The parameters specifying the traction-separation relationships are: normal and shear mode elastic stiffness,  $E_n = E_s = 2.0e6$  MPa, normal mode interface strength,  $T_n = 50$  MPa, shear mode interface strength,  $T_s = 80$  MPa, normal mode fracture energy,  $G_{nc} = 0.3$  MPa-mm, and shear mode fracture energy,  $G_{sc} = 1.5$  MPa-mm. The mixed mode fracture behavior in the CEs is specified using Benzeggagh-Kenane (BK) criterion with power,  $\eta = 1.8$ . The interaction between the impactor and the panel as well as between the plies of the panel after interfacial failure is specified through the general contact definition in Abaqus/Explicit. Furthermore, all contact interactions are considered frictionless. The analyses are conducted in double precision using Abaqus/Explicit code running on a Linux x86-64 machine. Two different impact velocity, 10 m/s and 50 m/s, are considered for the analyses.

### 4. Damage Formation and Growth under Dynamic Loading Conditions

Under impact loading condition both interfacial and internal damage mechanisms occur simultaneously within the material or structure. However, in many circumstances only interfacial damage mechanism is modeled and the internal damage mechanism is ignored or vice-versa, without proper justification. Thus, in the following, two cases are considered. In the first case, the

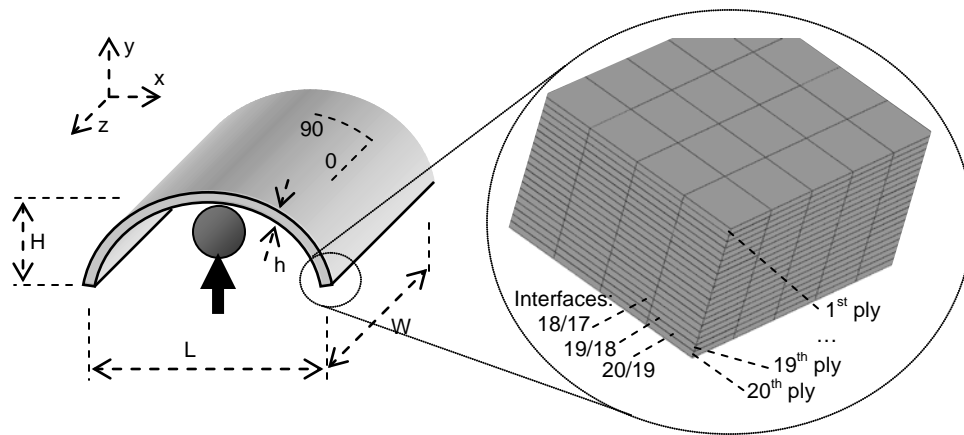


**Figure 3. Scheme of considered example and local segment of corresponding FEA model.**

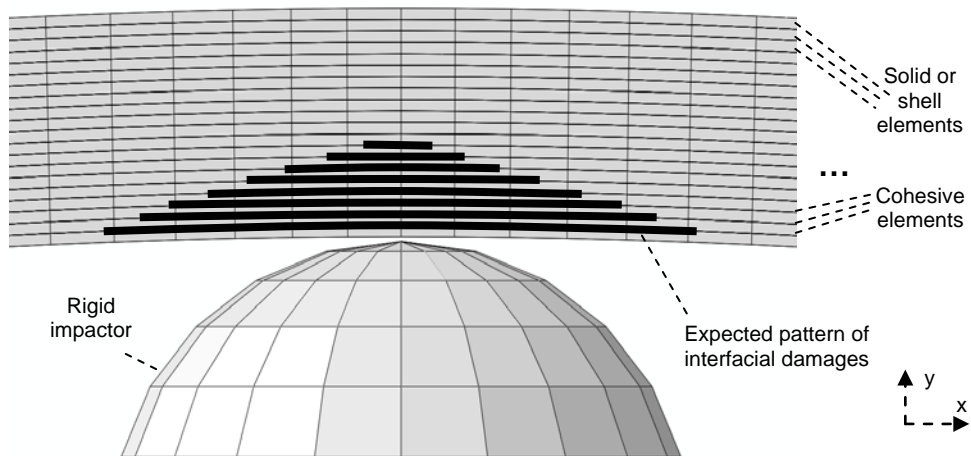


**Figure 4. Details of FEA implementation.**

internal damage modes are ignored and only interfacial damage mode is considered. Subsequently, both the damage modes are considered together in order to understand the coupling between the damage mechanisms and to assess whether ignoring certain damage modes in the analyses is justified.

#### 4.1 Single Damage Mechanism

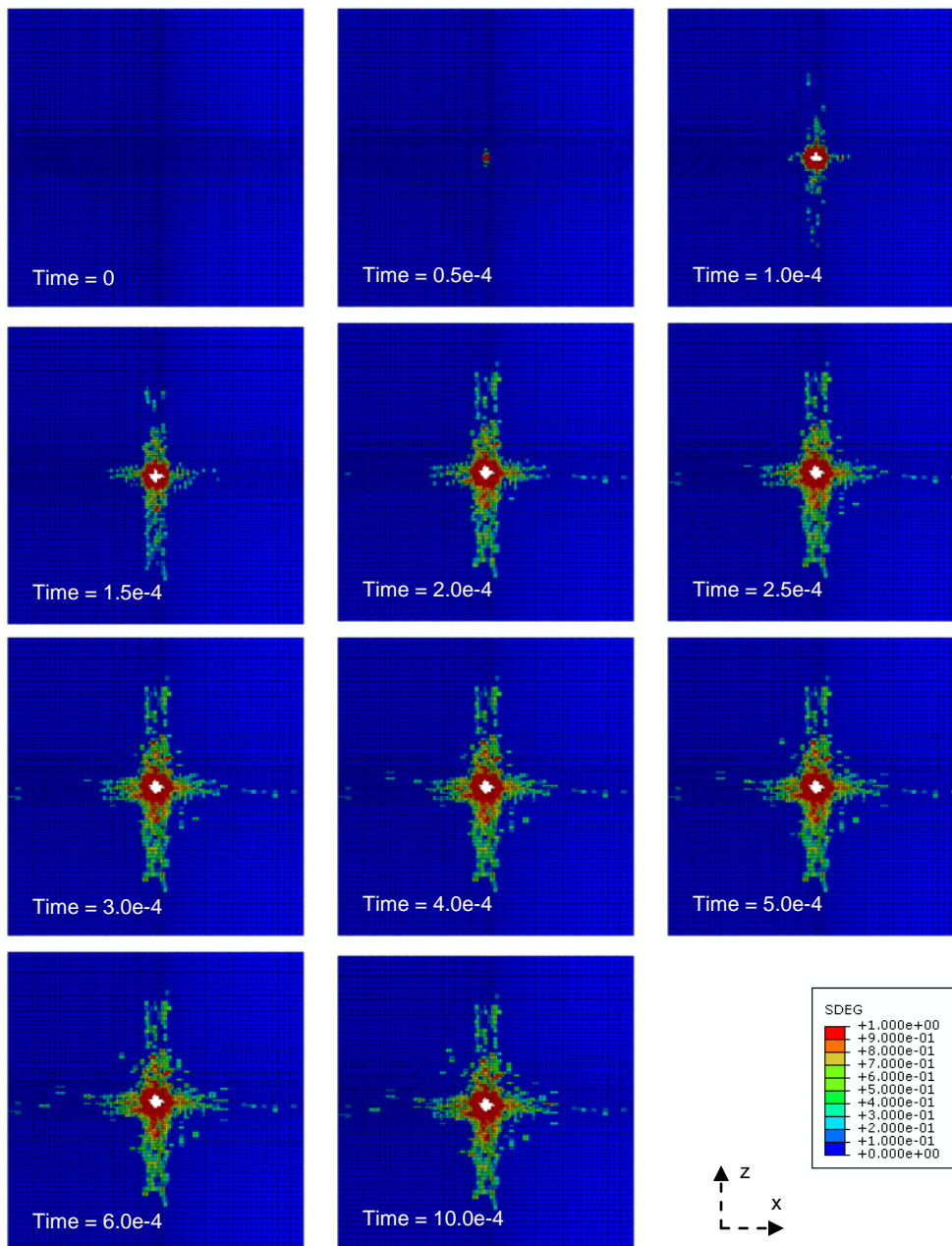
In this case the focus is on a single damage mechanism in isolation. This mechanism includes only interfacial damage processes between the plies. Thus, the plies are modeled as linear orthotropic elastic material without any internal damage evolution within them; the entire damage process consists of interfacial damage between the plies. The initiation and evolution of interfacial damage between the layers is modeled using cohesive elements in Abaqus/Explicit. Zero thickness CEs with matching nodes are embedded between each layer. Damage within CEs initiate once the maximum traction-based damage initiation criterion is met. Upon damage initiation the traction decreases until it reaches zero. Once the traction has become zero or, correspondingly, the damage parameter has reached 1.0, an interfacial separation (delamination) has occurred at that material point.

Figure 5 shows the time history of damage within the CEs at the interface closest to the impactor (interface between plies 19 and 20) for the impact velocity of 10 m/s. (the same legends for SDEG are applied to other figures, unless otherwise noted). It is seen that a small delamination is formed fairly early in the loading history, but it does not grow significantly. The damage in the surrounding CEs continues to grow with time until it reaches a steady state. However, it remains below 1.0 signifying that delamination has not formed. Similarly, at the impact velocity of 50 m/s the damage within the same interface was found to be considerably larger, as expected. For both impact velocities, the interfacial damage reduces in size as one moves to the ply interfaces away from the interface 20/19. The time-history of the impact force for both impact velocities is shown in Figure 6. In these figures, a comparison is made with the cases where both interfacial and internal damage mechanisms are ignored (i.e., a purely elastic solution) and where both damage mechanisms are considered (to be discussed next). It is evident that interfacial damage mechanism reduces the peak impact force when compared with purely elastic solution that ignores any damage mechanisms.

#### 4.2 Multiple Damage Mechanisms

The case of multiple damage mechanisms is considered next. In this case, the internal damage mechanisms occurring within the plies (matrix cracks, fiber breakage etc.) are modeled using the progressive damage model for fiber-reinforced composite materials in Abaqus/Explicit. In this model a Hashin failure criterion is used for damage initiation in various modes such as longitudinal tensile and compressive (fiber direction) and transverse tensile and compressive (matrix direction). Once the damage initiation has occurred an energy-based criterion is used for damage evolution in various modes. In Abaqus/Explicit complete failure of a material point occurs when fiber mode damage variables reach a user-specified maximum value (or a default value of 1.0). Furthermore, the element is considered fully damaged and removed from the mesh once the above criterion is satisfied at all the section points at one location within the element [1].

In this analysis a number of damage parameters are of interest. For interfacial damage the scalar damage parameter SDEG indicates the degree of damage within the CEs at ply interfaces. In addition, damage parameters representing internal damage within the plies are of interest. Here the damage parameter DAMAGESHR is shown for illustration. This damage parameter combines the different fiber and matrix damage modes and can be considered as an effective scalar internal damage parameter. Figure 7 gives the time history of interfacial damage parameter at ply interface



**Figure 5. Time evolution of interfacial damage parameter (SDEG) at ply interface 20/19 [impact velocity,  $v = 10$  m/s; without internal damage within the plies]**

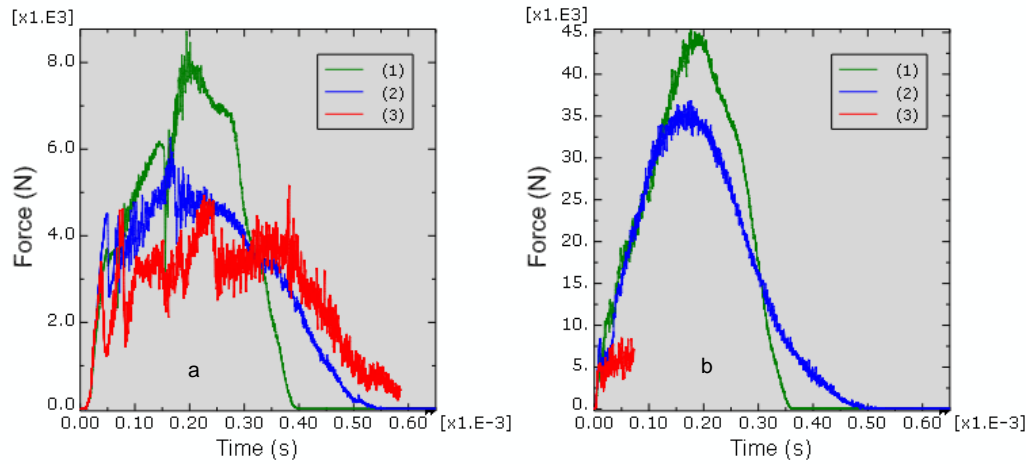


**Figure 6. Time history of overall impact force for impact velocity,  $v = 10$  m/s (a) and 50 m/s (b): (1) elastic solution, (2) only interfacial damage, and (3) interfacial and internal ply damage**

20/19 for the case of 10 m/s impact velocity. For the same impact velocity and at the end of simulation, the interface damage parameter at various ply interfaces is shown in Figure 8. The time history of internal damage parameter in the 19<sup>th</sup> ply is shown in Figure 9 and the value of the same parameter within various plies at the end of the simulation is shown in Figure 10. Note that Figure 9 is a zoomed-in view of the impact region.

A number of observations can be made from these figures. First, the interface damage and delamination patterns are similar to those observed in the case where no internal damage mechanisms were considered (Figure 5). Secondly, the size of delamination and associated interface damage is larger when compared with the case without internal damage. It may also be seen that some perforation of plies has occurred in the impact region for the impact velocity of 10 m/s. The ply damage is, however, more localized than the interfacial damage. Also note that both interface damage and ply internal damage reduce in size and intensity as one traverse away from the impact location in the +Y direction. Furthermore, the internal damage reduces more rapidly in the Y-direction than the interfacial damage.

The time history of the impact force for both impact velocities is superimposed with the earlier results in Figure 6. Note that for the case of 50 m/s impact velocity the analysis did not complete due to excessive distortion of the continuum shell elements in the close proximity of the impact site. For some reason one of the section points of the excessively distorted element did not reach the condition for complete damage, preventing that element from deletion. In any case, it may be noted that for both impact velocities consideration of multiple damage mechanisms leads to a lower peak impact force when compared with the case where only interfacial damage mechanism was considered. This is intuitively expected as multiple damage mechanisms allow for more damage pathways leading to larger damage dissipation and overall compliant structure.

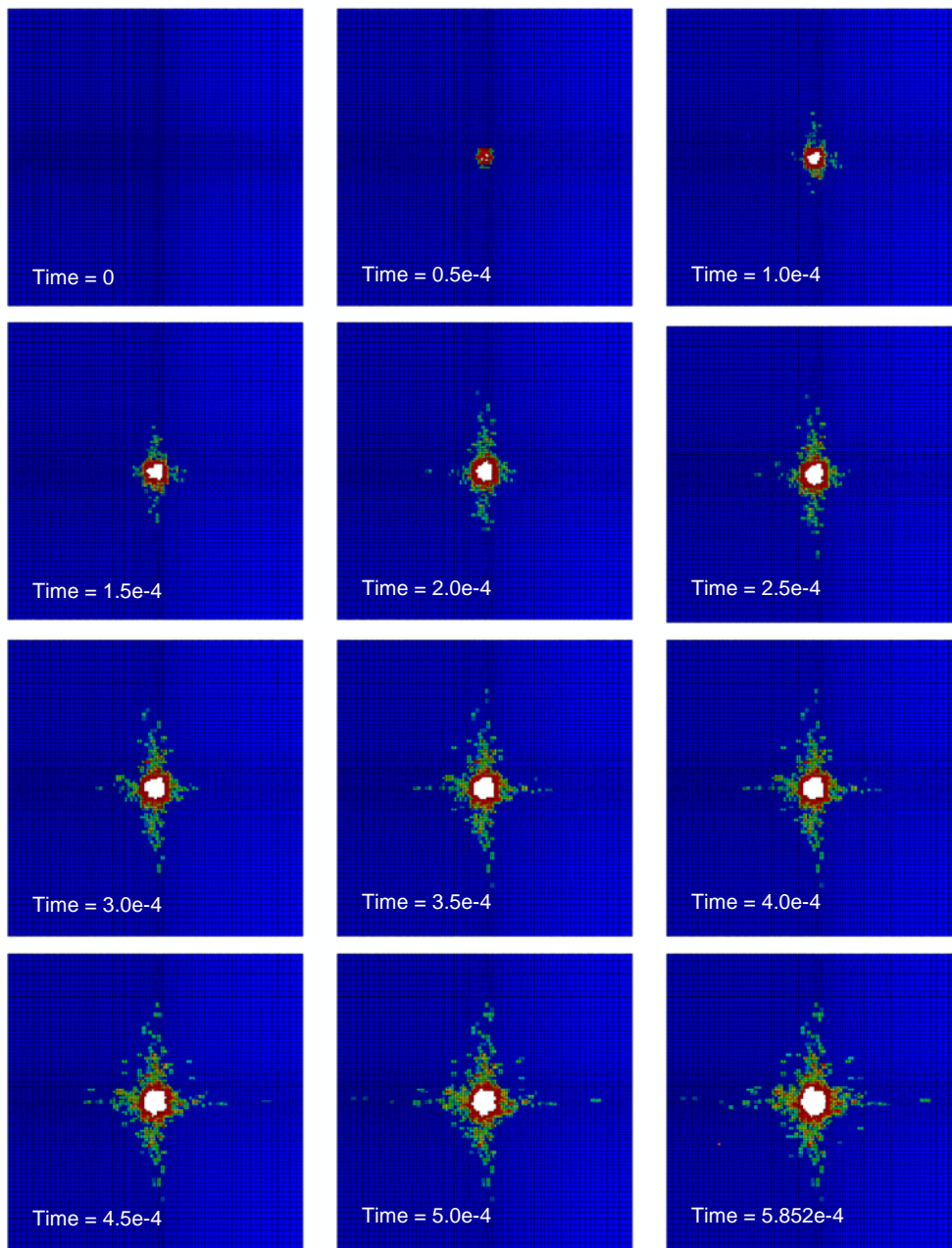


**Figure 7. Time evolution of interfacial damage parameter (SDEG) at ply interface 20/19 [impact velocity,  $v = 10$  m/s; with interfacial and internal ply damage]**

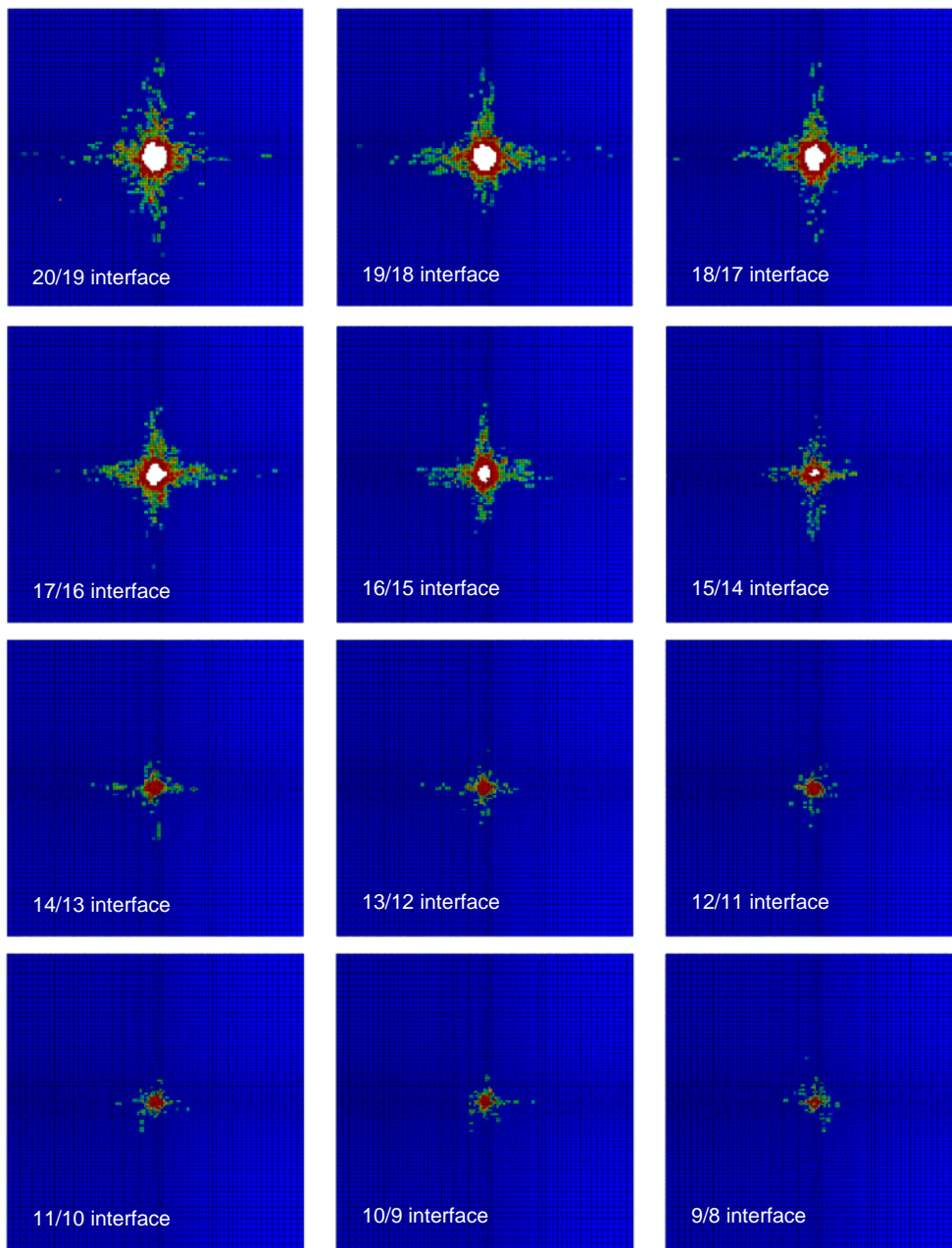


**Figure 8. Distribution of interfacial damage parameter (SDEG) at various ply interfaces at time = 5.852e-4 s [impact velocity,  $v = 10$  m/s; with interfacial and internal ply damage]**

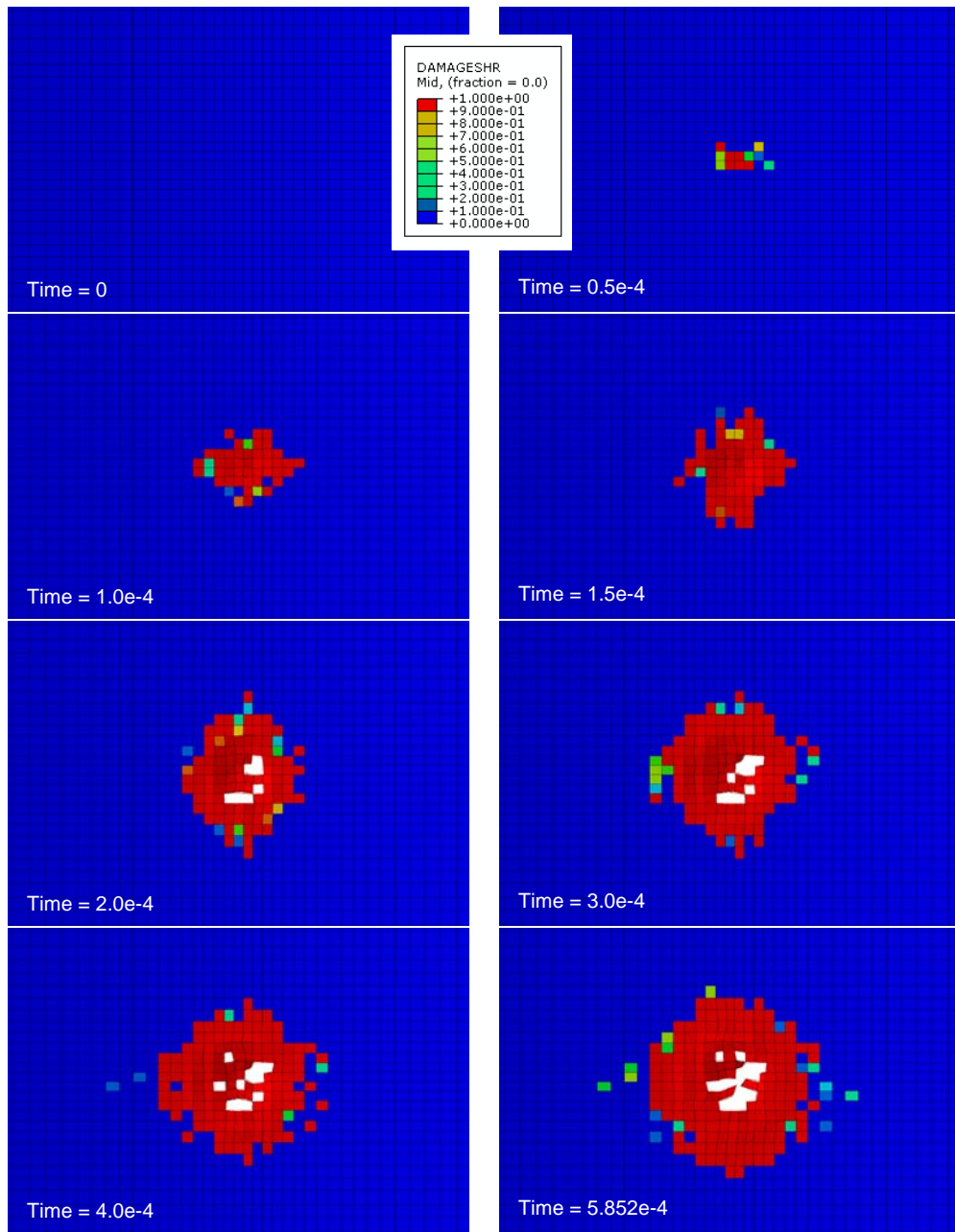


**Figure 9. Time evolution of internal ply damage parameter (DAMAGESHR) in ply 19 [impact velocity,  $v = 10$  m/s; with interfacial and internal ply damage]**

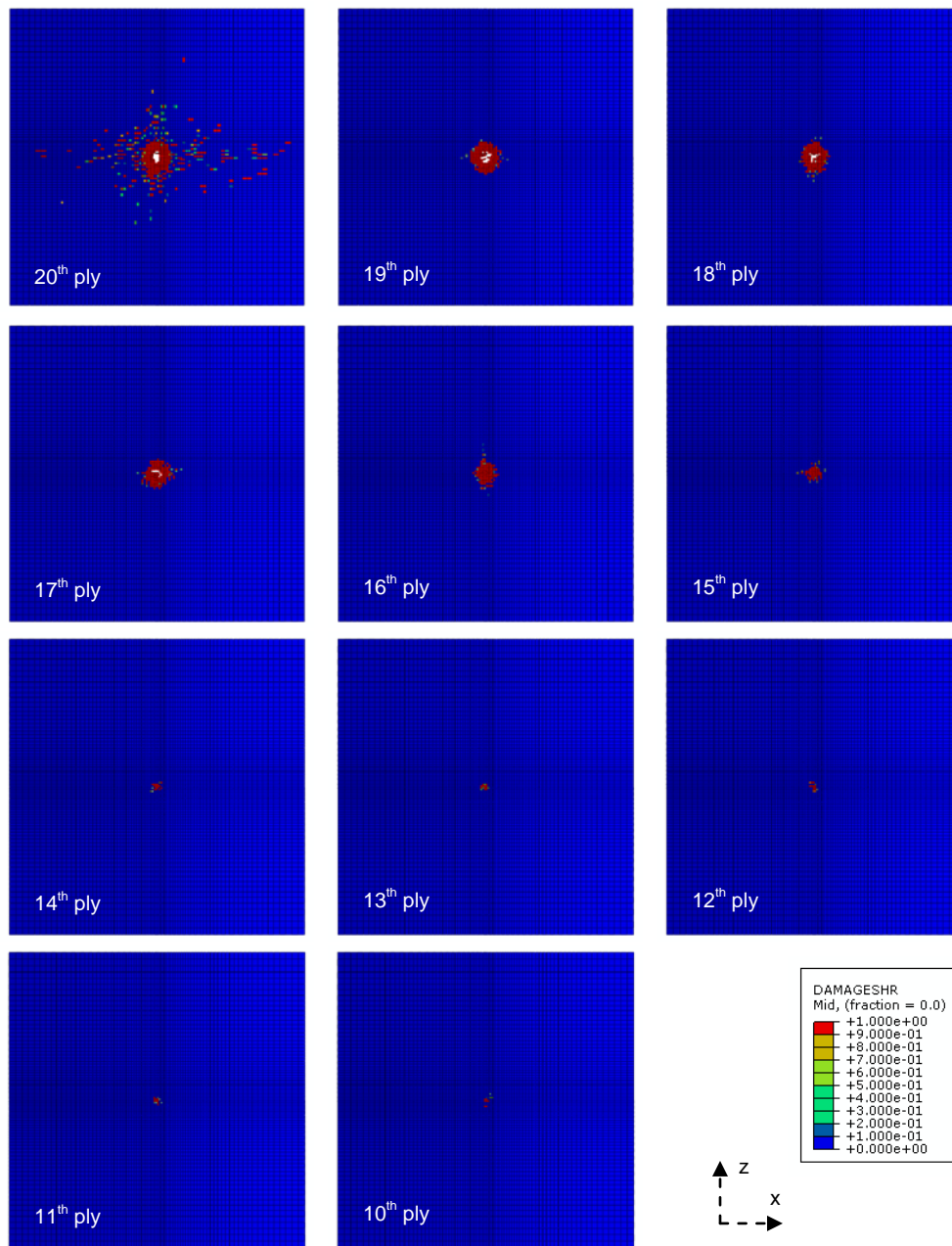


**Figure 10. Distribution of internal ply damage parameter (DAMAGESHR) in ply 19 at time = 5.852e-4 s [impact velocity,  $v = 10$  m/s; with interfacial and internal ply damage]**

The effect of impact velocity on interfacial damage for the case where internal ply damage is not considered can be noted from Figure 11. As expected, higher velocity would lead to more interface damage. For the case where internal ply damage is included in the analysis, it is expected that the interface damage would follow similar trend.

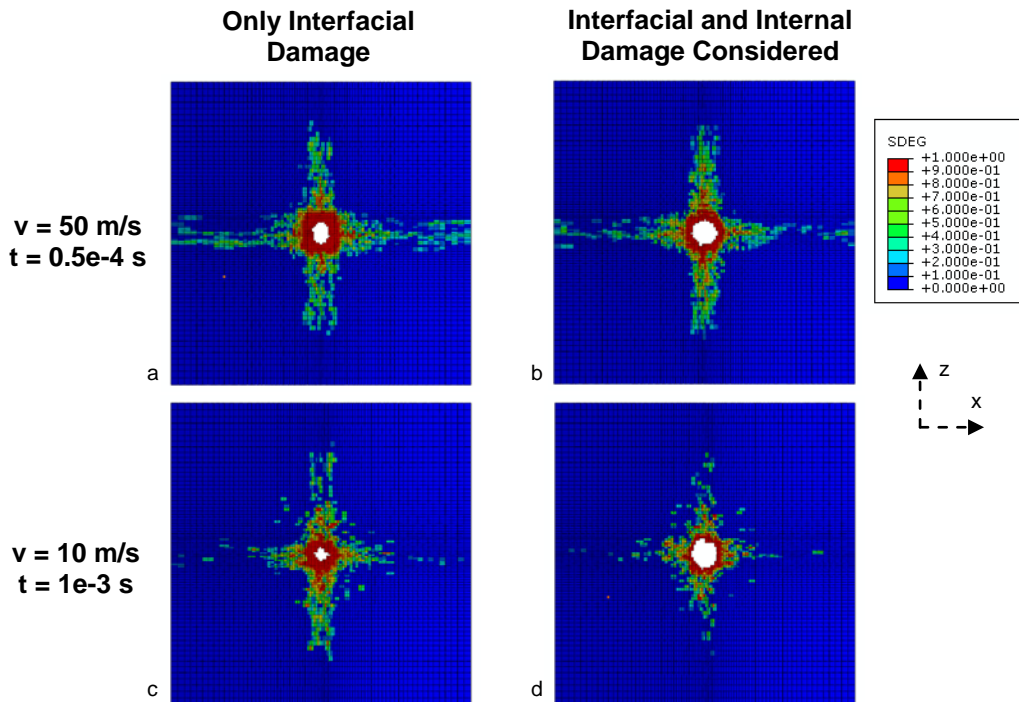


**Figure 11. Interfacial damage parameter (SDEG) at ply interface 20/19 predicted without and with internal ply damage.**

For the impact velocity of 10 m/s the interfacial damage size at interface 20/19 at the end of the simulation for the case where internal damage is not considered is compared against the case where internal ply damage is considered in Figure 11c,d. It is seen that consideration of internal damage within the plies leads to higher interfacial damage. This result is counter-intuitive as one might expect that ignoring internal damage mechanisms in plies would lead to higher interfacial damage as more energy is available for forming interfacial damage in this case. However, the simulation results point to a synergism between the interfacial and the internal damage mechanisms: by considering internal damage mechanisms in the plies leads to more interfacial damage. A similar conclusion can be noted for higher impact velocity (50 m/s) as shown in Figure 11a,b.

## 5. Effect of Element Selection and Comparison with LS-DYNA Solution

In computational simulations involving commercial FEA codes the analyst is faced with numerous modeling choices and options. These choices are usually based on analyst's experience, time constraints, and available capabilities within the codes, amongst others. For example, in the present study the choice of continuum shell elements to model the plies was dictated by the lack of a built-in progressive damage material model for fiber-reinforced composite materials for 3D solid elements in Abaqus. Even though a damage model for solid element is available as a user material model (VUMAT) in Abaqus/Explicit, it is different than the Hashin's progressive damage model. However, a limited study was conducted on the effect of the element type (continuum shell, SC8R versus solid, C3D8R) for the case where only interface damage was considered and the results will be discussed shortly.

Another aspect of computational analyses that is crucial in any engineering environment is robustness and correctness of the computational solution. In this work the modeling approach and results are assessed by comparing Abaqus/Explicit and LS-DYNA [2] solution for the case where only interfacial damage mechanism is allowed in the analysis.

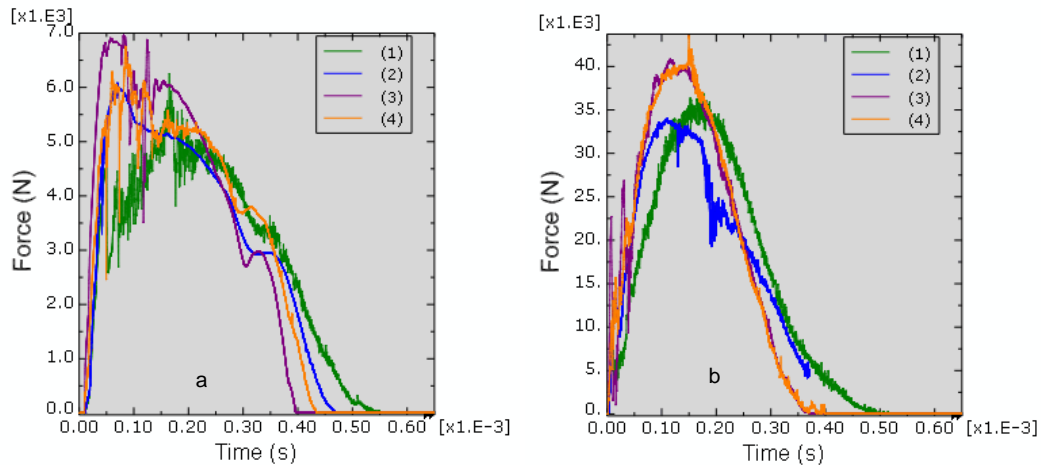


**Figure 12. Time history of overall impact force for impact velocity,  $v = 10$  m/s (a) and 50 m/s (b) when only interfacial damage considered: (1) Abaqus continuum shell, (2) Abaqus solid, (3) LS-DYNA thick shell, and (4) LS-DYNA solid elements**

The results from both these studies are compared in Figure 12 corresponding to impact velocity of 10 m/s and 50 m/s, respectively. It is seen that for  $v = 10$  m/s, both Abaqus solid element and LS-DYNA solid element leads to almost identical force-time response. The response of continuum shell (thick shell in LS-DYNA terminology) differs slightly from the solid response. However, all

the response characteristics still appear reasonable; the reason for the difference could be related to the mesh density, differences in bending behavior of solid versus thick shell, etc. For  $v = 50$  m/s LS-DYNA solid and thick shell response are almost identical, whereas, Abaqus solid and continuum shell response show slight difference even though the peak force is identical. At this stage the reasons for these differences are not clear. It should be worth mentioning that despite the minor differences in the overall force-displacement response, the interfacial damage patterns are similar in these cases, giving confidence in the simulation results.

## **6. Conclusions**

An efficient methodology is suggested and demonstrated for impact modeling of complex heterogeneous materials and structures. Reliable computational validation of the described methodology is demonstrated by comparison with corresponding independent LS-DYNA solutions as well as using different types of elements (continuum shell, solid elements). It is shown that the coupling between the internal and the interfacial damage mechanisms can be very important in understanding and characterization of actual material failure. The methodology seems to be a convenient way for numerous engineering applications involving impact behavior.

## **7. References**

1. Abaqus Analysis User's Manuals, v6.9, Dassault Systèmes SIMULIA Corp., 2009.
2. LS-DYNA User's Manuals, v971, Livermore Software Technology Corp., 2007.

## **8. Acknowledgement**

The authors thank *United Technologies Research Center* for permission to publish this paper.